Orbit Prediction in the Presence of Gravitational Anomalies

STEVEN ROY CROOPNICK*
MIT Charles Stark Draper Laboratory, Cambridge, Mass.

The classical description of a body's gravitational field is by means of an infinite series expansion in spherical harmonics, which lends itself well to most orbit determination problems. For low orbiting spacecraft, however, local gravitational anomalies have an effect on the path of a spacecraft which increases as the distance from the spacecraft to the body decreases. This paper develops an efficient, localized gravity model which uses suborbital surface distributions of mass and, a new gravity modeling tool, gravity dipoles on the surface of a body. Mathematical techniques are developed to calculate recursively the gravity field arising from this model. It is also shown that the tangential component of disturbing acceleration is approximately proportional to the derivative of the radial component for low circular orbits. Several numerical examples of these developments are presented.

Introduction

PRIOR to the advent of orbital space vehicles, the study of physical geodesy was supported by geodetic experiments performed on or near the surface of the Earth. Traditionally, the gravity models consisted of local descriptions of the gravity field and its potential or low-order expansions of the gravitational potential in spherical harmonics. Part of the difficulty in obtaining a more sophisticated model was that there were large areas where gravimetric data was impractical or impossible to obtain. Examples of these regions are the oceans and countries unfriendly to our government. The use of artificial Earth satellites had the effect of unifying the data and allowing one to solve simultaneously for the locations at which data was taken with respect to one another, satellite parameters and the coefficients of the Earth's potential expansion in spherical harmonics. This potential function is of the form

$$\Phi(\mathbf{r}) = \frac{GM}{r}\left[1 + \sum_{n=2}^{\infty}\left(\frac{r_e}{r}\right)^n \sum_{m=0}^{n} (C_{nm}\cos m\lambda + S_{nm}\sin m\lambda) P_{nm}(\sin L)\right] \quad (1)$$

where G is the gravitational constant, C_{nm} and S_{nm} are the gravitational coefficients, $\mathbf{r}$ is the position vector with respect to an Earth fixed frame, M is the mass of the Earth, r_e is its equatorial radius, λ the longitude, L the latitude and P_{nm} are the associated Legendre functions. There exist many ways of estimating these gravitational coefficients, depending on the type of data available. For example, the U.S. Navy Satellite Doppler System, Tranet, employs artificial near-Earth satellites whose range rate is measured from fixed ground stations. A typical pass over a ground station contains between 200–400 individual data points. This made possible the acquisition of a dense set of data which is ideally suited for studying the higher frequency effects of gravitational forces acting on a satellite. The Smithsonian Astrophysical Observatory also collects data from a number of sources which they independently process to solve for the gravitational coefficients. Some of their data input include photographs taken with Baker-Nunn cameras which yield satellite right ascension and declination at the time of the photograph, laser range data, data from the National Space Science Data Center (NSSDC), data from Tranet made available by the Applied Physics Laboratory, and range and range rate data obtained from the Goddard Space Flight Center.

This formulation of the gravitational potential would be exact if the expansion were carried out to an infinite number of terms. The form of the expansion indicates that the convergence for this representation of the potential is better for large values of r than for values close to r_e. In the case of the Earth, the effect of the higher order terms is small because a satellite never gets close to the surface due to the limitations of the atmosphere, so that a tenth- or fifteenth-order representation is adequate for most near-Earth applications.

Such is not the case for the moon, however. Separate studies performed at California Institute of Technology's Jet Propulsion Laboratory (JPL) and NASA's Langley Research Center (LRC) indicate that there are significant difficulties in modeling the moon's gravitation potential field in terms of spherical harmonics. The JPL study[1] analyzed data from Earth based radio tracking of Lunar Orbiters and raised doubts as to the validity of the data, the accuracy of the theoretical model, the completeness of the model and the behavior of the spacecraft. Attempts were made to correct the observed data for the perturbing forces (other than those due to gravity), the accuracy of the data due to radio signal effects, data processing errors and other potential error sources. After considering all these effects, the resulting Doppler data indicated large residual differences between the actual Doppler data and the expected or calculated Doppler data based on a fourth-order spherical harmonic moon gravity model. An example is presented in Fig. 1 of their large Doppler

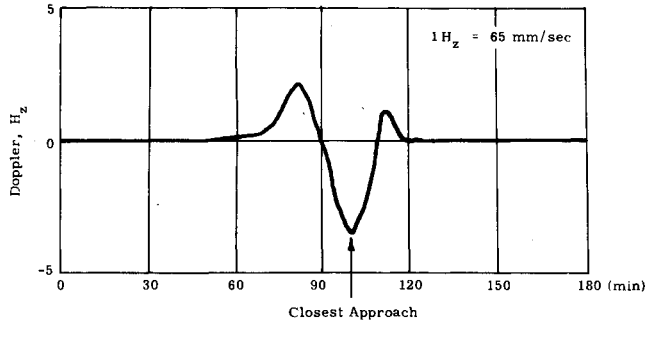

Fig. 1 Lunar Orbiter IV Doppler residuals, Goldstone, June 17, 1967.

Presented as Paper 71-375 at the AAS/AIAA Astrodynamics Conference, Fort Lauderdale, Fla., August 17–19, 1971; submitted September 8, 1971; revision received February 17, 1972. The research was sponsored by NASA through contract NAS-9-9024.

Index categories: Spacecraft Navigation, Guidance, and Flight-Path Control Systems; Lunar and Planetary Trajectories; Earth-Orbital Trajectories.

* Staff. Associate Member AIAA.

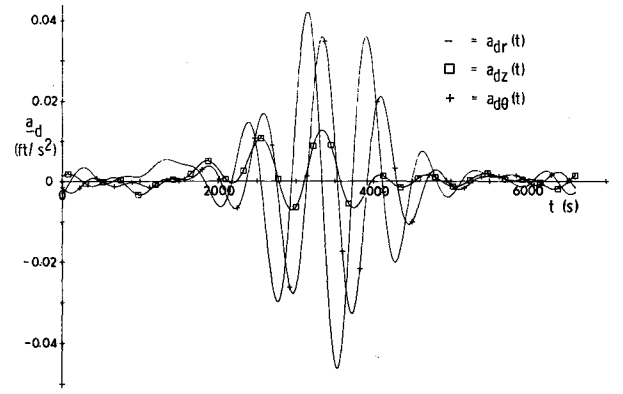

Fig. 2 Disturbing accelerations from a 13th-order lunar gravity field in spherical harmonics.

residuals that occur near pericenter for the Lunar Orbiter IV. Since these unexplained residuals occurred only at or near pericenter, it seemed reasonable to assume that they were caused by local unmodeled gravity anomalies. The LRC study[2] was performed independently and also questioned the occurrence of the rapid fluctuations of the Doppler residuals in the region of the Orbiter's pericenter. The residuals appeared to be independent of the location of Orbiter pericenter at the moon and of the particular tracking stations involved. The conclusion reached in this study was that the higher order gravity terms have a pronounced effect on the residuals in the region of satellite pericenter and must be included in the solution when sufficient data is available.

A physical explanation of the gravitational roughness of certain regions of the moon was given by Muller and Sjogren[3-5] at JPL. Noting that there were localized regions of strong, rapidly fluctuating Doppler residuals, which corresponded to lunar surface features known as ringed maria, they hypothesized the existence of localized lunar mass concentrations (mascons) within the ringed maria. By adjusting the size and depth of these mascons, they were able to account for the large Doppler residuals. This modeling concept was studied by P. Gottlieb at JPL and L. Wong at the Aerospace Corporation and is reported on in Refs. 6 and 7.

The desirability of having a surface distribution of mass and dipoles which may be adjusted easily to model the local disturbing acceleration, is made evident from an examination of Fig. 2. A 10-mile circular equatorial orbit around the moon was simulated using a thirteenth-order model of its gravity field supplied by Langley Research Center. The simulation starts at 0° latitude, 0° longitude, which is a point in the center of the front surface of the moon as viewed from Earth, and made one complete orbit. The large disturbing accelerations, which correspond to the backside region of the moon, are an order of magnitude larger than the disturbing accelerations which correspond to the frontside. One possible explanation for the large discrepancy in the magnitudes of the disturbing accelerations is that they result from fitting data taken only near the frontside of the moon, and not on the backside. The form of the expansion of the lunar potential in spherical harmonics makes it difficult to make local changes in the gravity field without affecting the field elsewhere as would be possible by modeling local surface mass anomalies directly.

The unmodeled mass distributions offered an explanation of the Doppler residuals. This paper investigates a suborbital distribution of mass and of gravity dipoles. A ring of mass whose density varies along the track is provided to produce the in-plane components of the disturbing accelerations. The out-of-plane disturbing accelerations are produced by a distribution of gravitational dipoles. This new[8] concept in modeling gravity fields is useful because it approximates the field caused by a relatively high-mass density region close to a low-density region, the properties of which are presented herein. The philosophy behind this new model is straightforward: the model proposed corresponds directly to the presumable causes of the gravity anomalies, and is of the form

$$\mathbf{a}_d(\mathbf{r}) = \mathbf{i}_r\left[\sum_{n=0}^{\infty}(\alpha_n\cos n\theta+\beta_n\sin n\theta)R_n'(r)\right]s_r(r)+$$
$$\mathbf{i}_\theta\frac{1}{r}\left[\sum_{n=0}^{\infty}(-\alpha_n n\sin n\theta+\beta_n n\cos n\theta)R_n(r)\right]s_\theta(r)+$$
$$\mathbf{i}_z\frac{1}{[r^2+r_0{}^2]^{3/2}}\left[\sum_{n=0}^{\infty}(a_n\cos n\theta+b_n\sin n\theta)H_n(r)\right]s_z(r) \qquad (2)$$

where $\mathbf{i}_r$, $\mathbf{i}_\theta$, and $\mathbf{i}_z$ are unit vectors in the r, θ, and z directions, respectively, θ is the central angle describing the in-plane position of the body at $\mathbf{r}$, the terms $R_n(r)$ and $H_n(r)$ are functions that produce the r dependence of the nth harmonic of $\mathbf{a}_d(\mathbf{r})$, the α's, β's, a's and b's are the new gravity coefficients and the s functions are normalizing coefficients. The number of terms for representation through the nth harmonic of a gravity field in spherical harmonics is $n(n+1)$, while the corresponding number of terms is only $4(n+1)$ for the new gravity model. This reduction is possible because the new model provides only a local description of the gravity field, whereas spherical harmonics provides a global description.

Analytical Implementation of New Gravity Models

Gravity Dipoles

A gravitational dipole[8] is a vector quantity $\mathbf{P} = md\mathbf{i}_d$ produced by a positive mass m, separated from a negative mass $-m$ by a distance d, in the limit as $d \to 0$ keeping the product md constant. The point dipole has a magnitude md and a direction from the negative mass to the positive mass. Its field may be derived by taking the gradient of its potential.

The gravitational potential at $\mathbf{r}$ due to a point dipole located at $\mathbf{r}'$ is

$$\Phi_d(\mathbf{r}) = G[md(\mathbf{r}-\mathbf{r}')\cdot\mathbf{i}_d/|\mathbf{r}-\mathbf{r}'|^3] \qquad (3)$$

so that

$$\nabla\Phi_d(\mathbf{r}) = G[\mathbf{P}-3(\mathbf{P}\cdot\mathbf{n})\mathbf{n}/|\mathbf{r}-\mathbf{r}'|^3] \qquad (4)$$

where $\mathbf{n}$ is a unit vector in the direction of $\mathbf{r}-\mathbf{r}'$.

Although gravity dipoles have never been shown to exist physically, they may be used effectively as modeling tools to change local gravity features without changing the net mass. An example of the type mass distribution that they could model would be a mountain next to a valley as shown in Fig. 3. The mountain would represent + mass while the valley, a distance $-\mathbf{d}$ away, would represent the − mass, both with respect to the average local mass density. The parameters available for use as modeling tools are the strength of the dipole, its direction and its location.

Equatorial Gravity Model

A common spacecraft orbit about a distributed mass is a circular orbit in the equatorial plane of the body. For this geometry the in-plane disturbing accelerations are modeled as those arising from a suborbital ring of mass. The distribution of the mass in the ring will be adjusted to fit, in some sense, the disturbing acceleration, or some measurable components of it during a flight. The out-of-plane components of the disturbing acceleration are modeled by an appropriate suborbital distribution of gravity dipoles in the form of a continuous line distribution around the equator. All the dipoles are oriented

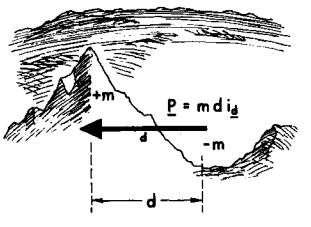

Fig. 3 Physical representation of a gravity dipole.

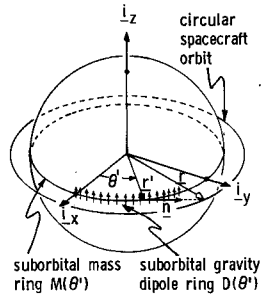

Fig. 4 Equatorial gravity model.

normal to the equatorial plane so that the net disturbing acceleration produced by their sum nominally results in only an out-of-plane component (see Fig. 4). The potential of a distributed mass ring with a line mass density $M(\theta')$ is given by

$$\Phi_m(\mathbf{r}) = G\int_0^{2\pi} \frac{M(\theta')r_0}{|\mathbf{r}-\mathbf{r}'|}d\theta' \tag{5}$$

where r_0 is the equatorial radius of the body. The in-plane components of the disturbing acceleration may be obtained from Eq. (5) by taking its gradient and expanding the result in a Fourier series

$$\mathbf{A}_{dm}(\mathbf{r}) = \mathbf{i}_r\left[\sum_{n=0}^{\infty}(\alpha_n\cos n\theta+\beta_n\sin n\theta)R_n'(r)\right]+ \mathbf{i}_\theta\frac{1}{r}\left[\sum_{n=0}^{\infty}(-\alpha_n n\sin n\theta+\beta_n n\cos n\theta)R_n(r)\right] \tag{6}$$

where the α's and β's are given constant gravity coefficients and the transfer functions $R_n(r)$ and $R_n'(r)$ are functions of r_0 and r only. For $n=0$, only the first α_n term contributes to $\mathbf{A}_{dm}$, hence for an nth order representation of the mass distribution, Eq. (6) will require $2n+1$ terms to give an in-plane description of the disturbing acceleration. Evaluation of the transfer functions is based on a class of functions of the form

$$G_n(k) = \int_0^{2\pi}\frac{\cos n\phi\, d\phi}{[1+k\cos\phi]^{1/2}} \tag{7}$$

where

$$R_n(r) = G_n(k)/[r^2+{r_0}^2]^{1/2};\quad k=-2rr_0/(r^2+{r_0}^2) \tag{8}$$

and

$$R_n'(r) = \{1/[r^2+{r_0}^2]^{5/2}\}\times [-r(r^2+{r_0}^2)G_n(k)+2r_0(r^2-{r_0}^2)G_n'(k)] \tag{9}$$

Although it is theoretically possible to develop recursive relationships for $G_n(k)$ $n\geqq 2$, it is expedient to introduce an auxiliary function defined as

$$N_n(k) = \int_0^{2\pi}\frac{\cos^n\phi\, d\phi}{[1+k\cos\phi]^{1/2}} \tag{10}$$

which may be evaluated from the specific elliptic integrals[9] $E(2\pi,h)$ and $F(2\pi,h)$ where $h^2=2k(1+k)^{-1}$. It is interesting to note[8] that E and F are also hypergeometric functions so that a simple method of finding their derivatives could be employed. The function $G_n(k)$ may be obtained from lesser order $N_n(k)$ functions as may their derivatives

$$G_n(k) = \sum_{i=0}^{n} f(n,i)N_{n-2i}(k) \tag{11}$$

and

$$G_n'(k) = \sum_{i=0}^{n} f(n,i)N_{n-2i}'(k) \tag{12}$$

where

$$f(n,i) = (-1)^i 2^{(n-1-2i)}n(n-1-i)!/i!\,(n-2i)! \tag{13}$$

and terminates when $(n-2i)=0$ or 1. The recursion relationships for the $N_n(k)$ and $N_n'(k)$ functions are

$$N_n(k) = [1/(2n-1)]\{-[2(n-1)/k]N_{n-1}(k)+(2n-3)N_{n-2}(k)+[2(n-2)/k]N_{n-3}(k)\} \tag{14}$$

and

$$N_n'(k) = [1/2(n-1)]\{[-2(n-1)/k]N_{n-1}'(k)+[2(n-1)/k^2]N_{n-1}(k)+(2n-3)N_{n-2}'(k)+[2(n-2)/k]N_{n-3}'(k)-[2(n-2)/k^2]N_{n-3}(k)\} \tag{15}$$

To start these recursion relationships, the values of $N_0(k)$, $N_1(k)$, $N_2(k)$ are needed to find $N_n(k)$ and ultimately $G_n(k)$, while $N_0'(k)$, $N_1'(k)$, and $N_2'(k)$ in addition, are needed to find $N_n'(k)$ and ultimately $G_n'(k)$. The terms $N_0(k)$ and $N_1(k)$ are identically equal to $G_0(k)$ and $G_1(k)$, respectively,

$$N_0(k) = G_0(k) = \int_0^{2\pi}(1+k\cos\phi)^{-1/2}\,d\phi \tag{16}$$

and

$$N_1(k) = G_1(k) = \int_0^{2\pi}\cos\phi\,(1+k\cos\phi)^{-1/2}\,d\phi \tag{17}$$

The $N_2(k)$ term may also be expressed as a function of k, $N_0(k)$, and $N_1(k)$ as

$$N_2(k) = \tfrac{1}{3}[N_0(k)-(2/k)N_1(k)] \tag{18}$$

The derivative terms may be obtained by simply differentiating Eqs. (16–18) with respect to k

$$N_0'(k) = G_0'(k) \tag{19}$$

$$N_1'(k) = G_1'(k) \tag{20}$$

and

$$N_2'(k) = \tfrac{1}{3}[G_0'(k)+(2/k^2)G_1(k)-(2/k)G_1'(k)] \tag{21}$$

In summary, $\mathbf{A}_{dm}(r)$ may be calculated for any r and θ and a given n, from Eq. (6), where the α_n's and β_n's are also given and where the $R_n(r)$ and $R_n'(r)$ functions are calculated according to Eqs. (8) and (9), respectively. The functions $G_n(k)$ and $G_n'(k)$, for k given by Eq. (8), are calculated from Eqs. (11) and (12), respectively. The terms involved in evaluating these equations are calculated recursively with the aid of Eqs. (14) and (15). The basis for the initiation of these equations is the calculation of $G_0(k)$, $G_1(k)$, $G_0'(k)$, and $G_1'(k)$. The expressions for the calculation of these functions are found in the Appendix. Numerical evaluation of the family of $N_n(k)$ functions is straightforward since they are well behaved as shown in Fig. 5.

For the case of a spacecraft in a low equatorial orbit, the out-of-plane disturbing accelerations are modeled as those arising from a suborbital ring of gravity dipoles. The potential of this ring with a line dipole density $\mathbf{D}(\theta')$ may be developed in a fashion similar to the mass ring:

$$\Phi_d(\mathbf{r}) = Gr_0\int_0^{2\pi}\frac{\mathbf{D}(\theta')\cdot(\mathbf{r}-\mathbf{r}')}{|\mathbf{r}-\mathbf{r}'|^3}d\theta' \tag{22}$$

The dipoles are oriented in the z direction so that their contribu-

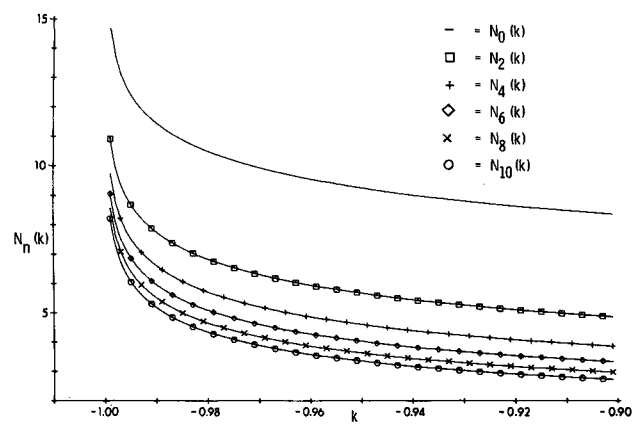

Fig. 5 Family of $N_n(k)$ functions.

tion to the disturbing acceleration is normal to the orbital plane, hence,

$$\mathbf{D}(\theta') = D(\theta')\mathbf{i}_z \tag{23}$$

so that the z component of the disturbing acceleration is then calculated as follows:

$$\mathbf{A}_{dd}(\mathbf{r}) = \frac{\mathbf{i}_z}{[r^2+r_0^2]^{3/2}} \sum_{n=0}^{\infty} H_n(k)[a_n \cos n\theta + b_n \sin n\theta] \tag{24}$$

where $H_n(k)$ is defined as:

$$H_n(k) = \int_0^{2\pi} \frac{\cos n\phi}{[1+k\cos\phi]^{3/2}} d\phi \tag{25}$$

Substitution of Eqs. (11–13) into Eq. (25) yields a convenient method for calculating $H_n(k)$ from the $N_n'(k)$ functions, which have been calculated previously

$$H_n(k) = -2 \sum_{i=0}^{n'} f(n,i) N'_{n-2i-1}(k) \qquad (n \geqq 1) \tag{26}$$

and terminates when $(n-2i) = 0$ or 1. The case for $n = 0$ cannot be handled by the general rule because $N'_{-1}(k)$ has not been defined. This case is solved separately

$$H_0(k) = -2N_1'(k) - (2/k)N_1(k) \tag{27}$$

The net result is that the disturbing acceleration due to the suborbital dipoles may be obtained from functions which were evaluated while calculating the disturbing accelerations from a suborbital mass ring.

Part of the difficulty encountered when modelling the gravitational field of a continuous distribution of mass by discrete or line masses is that the field becomes infinitely large as a mass point is approached. Attempts to circumvent this situation have been made by Gottlieb[6] and Wong.[7] Gottlieb expanded the field due to a point mass in a truncated spherical harmonic series while Wong placed the mass points below the surface of the body. The approach taken here is to scale each component of the disturbing acceleration to give the same field that would be produced by the suborbital masses and dipoles if they were uniformly distributed on the surface of the body.

Results and Conclusions

The effectiveness of the new gravity model may be examined by means of a comparison with another model whose properties are well known. Hence, as a basis for comparison, the gravitational potential of the Earth expressed in spherical harmonics was used. The harmonic coefficients used in this model were taken from a tenth order model given in Ref. 10 which consists of 110 terms.

The disturbing accelerations due to this gravity model are then compared to an "equivalent" representation of the disturbing accelerations produced by a suborbital distribution of mass and gravity dipoles, the coefficients of which are given in Ref. 8.

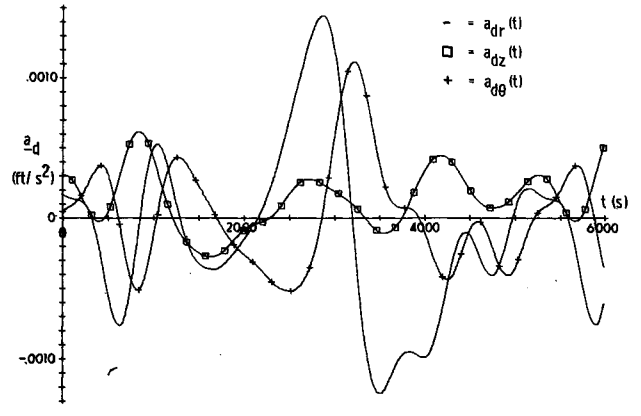

Fig. 6 Disturbing acceleration during one orbit derived from spherical harmonics.

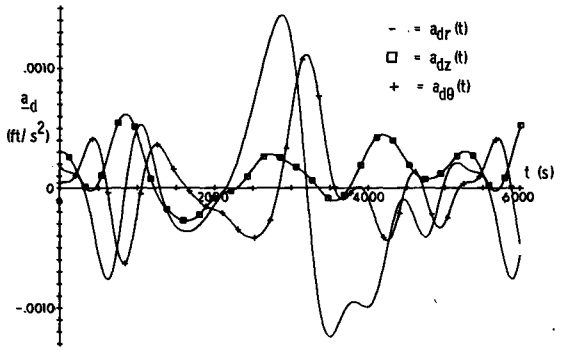

Fig. 7 Disturbing acceleration during one orbit derived from a suborbital mass and dipole ring.

The orbit selected for this comparison was a 100 mile circular equatorial orbit which is a common orbit, representative of the anticipated useful application of the new gravity model. The disturbing accelerations produced by the spherical harmonics model and the new gravity model are shown in Figs. 6 and 7, respectively. From an examination of these three components of disturbing acceleration, it may be seen that the actual disturbing accelerations along a low-altitude orbit may be successfully modeled by a suborbital distribution of mass and gravitational dipoles, such that the mass distributions account for the radial and tangential (in-plane) components of the disturbing acceleration while the dipoles account for the out-of-plane components. The motivation for developing these surface models directly is that the disturbing accelerations for low-altitude orbits are influenced relatively strongly by local mass anomalies due to the $1/r^2$ force law. This model is an attempt to account more realistically and effectively for local gravity anomalies affecting a low-orbiting vehicle. Therefore, this model is suited for low altitude, low-eccentricity orbits that fly over the same terrain repeatedly, such as a low-circular equatorial orbit. For the example presented here, it was found that the new model had a 3.2×10^{-5} ft/sec^2 mean absolute error. The error increased to 6.6×10^{-5} ft/sec^2 for an increase in altitude to 500 miles, and 5.9×10^{-5} ft/sec^2 for an out-of-plane excursion of 300 miles.

The number of coefficients needed for an nth-order representation of the disturbing acceleration utilizing the new gravity model is $4(n+1)$ as compared with $n(n+1)$ for spherical harmonics. The computation time needed to calculate the disturbing acceleration for each representation is approximately proportional to the number of coefficients in each model. If the computation time per coefficient were the same for each model, the new model would have the advantage of a linearly increasing computation time compared to one that increased quadratically with the order of the expansion as in the spherical harmonic representation. For a twentieth-order model, this amounts to approximately a five fold savings in computation time to produce $\mathbf{a}_d$ by using the new model instead of spherical harmonics. The limitation of the new model is that it may be used only for restricted regions, as opposed to the global properties of spherical harmonics.

A comparison of the computation time of the two methods of producing $\mathbf{a}_d$ may be made on a term by term basis. The factor that multiplies each coefficient using the expansion in spherical harmonics is

$$(r_e/r)^n \sin m\theta \, P_{nm}(\cos\phi)$$

or

$$(r_e/r)^n \cos m\theta \, P_{nm}(\cos\phi)$$

while the equivalent factor for the new model is $R_n(r)$, or $H_n(r)$ times $\sin m\theta$ or $\cos m\theta$. The $H_n(r)$ factor was shown to result as a by-product while calculating $R_n(r)$ or $R_n'(r)$ so that little time is consumed in producing it. The comparison therefore lies between $(r_e/r)^n P_{nm}(\cos\phi)$ and the R functions. Both functions are produced recursively from simple starting points which involve about the

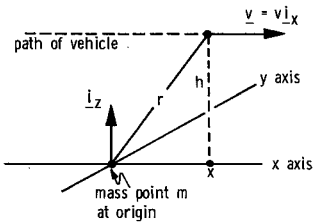

Fig. 8 Vehicle in free fall passing over a mass point.

same amount of complexity, and accordingly, the same amount of computer time.

Associated with the new gravity model are various mathematical developments. These include the representation of disturbing accelerations by gravitational dipoles, the transfer functions $R_n(r)$ and $R_n'(r)$, and the supporting G_n, G_n', N_n, N_n', and H_n functions. It was also noted in all cases that the theta component of the disturbing acceleration is approximately proportional to the negative derivative of the radial component. Although it is shown not to be an exact relationship, nonetheless, it appears as a reliable, quick check to see if plots of $\mathbf{a}_d$ seem reasonable. Some physical insight into this effect may be obtained by considering the geometry depicted in Fig. 8. The disturbing acceleration on the vehicle due to the mass point m at location $(0,0)$ is

$$\mathbf{a}_d(x) = -[Gmx/(x^2+h^2)^{3/2}]\mathbf{i}_x - [Gmh/(x^2+h^2)^{3/2}]\mathbf{i}_z = a_{dx}\mathbf{i}_x + a_{dz}\mathbf{i}_z \quad (28)$$

so that

$$a_{dx} = -Gmx/(x^2+h^2)^{3/2} \quad (29)$$

and

$$da_{dz}/dx = +3Gmhx/(x^2+h^2)^{5/2} \quad (30)$$

If x is small compared to h, the negative derivative of a_{dz}, which corresponds to a_{dr}, is approximately proportional to a_{dx} which corresponds to $a_{d\theta}$, hence, the derivative relationship is fairly well approximated over the linear range of $a_{dx}(x)$. For larger values of x, the denominator terms for a_{dx} and da_{dz}/dx go as r^3 and r^5, respectively, and therefore make the mismatch in their dependence on x less important. The importance of the denominator mismatch is further lessened because the region that the spacecraft is over generally has a stronger immediate influence on its motion than regions over which it has previously passed. Hence, the theta component of the disturbing acceleration is approximately proportional to the negative derivative of the radial component for low-circular orbits, as also seen in Figs. 6 and 7.

Appendix

The functions $G_0(k)$, $G_1(k)$, $G_0'(k)$, and $G_1'(k)$ may be calculated from the elliptic integrals $E(2\pi,h)$, $F(2\pi,h)$ and their derivatives as follows:

$$G_0(k) = (1+k)^{-1/2}F(2\pi,h)$$

$$G_1(k) = k^{-1}(1+k)^{1/2}E(2\pi,h) - k^{-1}(1+k)^{-1/2}F(2\pi,h)$$

$$G_0'(k) = (1+k)^{-1/2}[dF(2\pi,h)/dh]\,dh/dk - \tfrac{1}{2}(1+k)^{-3/2}F(2\pi,h)$$

$$G_1'(k) = \tfrac{1}{2}k^{-1}(1+k)^{-1/2}E(2\pi,h) + k^{-1}(1+k)^{1/2}[dE(2\pi,h)/dh]\,dh/dk - k^{-2}(1+k)E(2\pi,h) - k^{-1}(1+k)^{-1/2}[dF(2\pi,h)/dh]\,dh/dk + k^{-2}(1+k)^{-1/2}F(2\pi,h) + \tfrac{1}{2}k^{-1}(1+k)^{-3/2}F(2\pi,h)$$

where

$$h^2 = 2k/(1+k)$$

References

[1] Lorell, J. and Sjogren, W. L., "Lunar Orbiter Data Analysis," TR 32-1220, Nov. 15, 1967, Jet Propulsion Lab., Pasadena, Calif.

[2] Tolson, R. H. and Gapcynski, J. P., "An Analysis of the Lunar Gravitational Field as Obtained from Lunar Orbiter Tracking Data," presented at the IQSY/COSPAR Assemblies, London, England, July 17–28, 1967, NASA.

[3] Muller, P. M. and Sjogren, W. L., "Consistency of Lunar Orbiter Residuals with Trajectory and Local Gravity Effects," TR 32-1307, Sept. 1, 1968, Jet Propulsion Lab., Pasadena, Calif.

[4] Muller, P. M. and Sjogren, W. L., "Mascons: Lunar Mass Concentrations," *Science*, Vol. 161, Aug. 16, 1968, pp. 680–684.

[5] Muller, P. M., "Consistency of Lunar Orbiter Residual with Trajectory and Local Gravity Effects," Paper 68-131, Sept. 3–5, 1968, American Astronautical Society.

[6] Gottlieb, P., "Detailed Representation of Accelerations by Discrete Masses Represented by Spherical Harmonics," TM 311-70, Sept. 19, 1968, Jet Propulsion Lab., Pasadena, Calif.

[7] Wong, L., "Dynamical Determination of Mascons on the Moon," Rept. ATR-69(7140)-1, 1969, The Aerospace Corp., El Segunda, Calif.

[8] Croopnick, S. R., "Orbit Prediction in the Presence of Gravitational Anomalies," Ph.D. thesis-536, June 1970, MIT Charles Stark Draper Lab., Cambridge, Mass.

[9] Dwight, H. B., *Tables of Integrals and Other Mathematical Data*, MacMillan, New York, 1961.

[10] Lundquist, C. A., "Geodetic Satellite Results During 1967," Special Rept. 264, 1967, Smithsonian Astrophysical Observatory, Cambridge, Mass.

[11] Battin, R. H., *Astronautical Guidance*, McGraw-Hill, New York, 1964.

[12] Gapcynski, J. P., Blackshear, W. T., and Compton, H. R., "The Lunar Gravitational Field as Determined from the Tracking Data of the Lunar Orbiter Series of Spacecraft," Paper 68-132, Sept. 3–5, 1968, American Astronautical Society.

[13] Gottlieb, P., "Estimation of Local Lunar Gravity Features," IAU URSI Symposium on Planetary Atmospheres and Surfaces, Aug. 12, 1969.

[14] Heiskanen, W. A. and Moritz, H., *Physical Geodesy*, W. H. Freeman and Co., San Francisco, 1967.

[15] Lorell, J. and Sjogren, W. L., "Lunar Gravity: Preliminary Estimates from Lunar Orbiter," *Science*, Vol. 159, Feb. 9, 1968, pp. 625–627.

[16] Abramowitz, M. and Stegun, A., *Handbook of Mathematical Functions*, Dover Publications, New York, 1965.